EX/P6-5

Analysis of Pedestal Characteristics in JT-60U H-mode Plasmas Based on Monte-Carlo Neutral Transport Simulation

Y. Nakashima1), Y. Higashizono1), H. Kawano1), H. Takenaga2), N. Asakura2), N. Oyama2), and Y. Kamada2)

1) Plasma Research Center, University of Tsukuba, 1-1-1 Tennoudai, Tsukuba, Ibaraki 305-8577, Japan
2) Japan Atomic Energy Agency, Naka Fusion Institute, 801-1 Mukouyama, Naka 311-0193, Japan

e-mail contact of main author: nakashma@prc.tsukuba.ac.jp

Abstract. This paper describes the results of pedestal characteristics in H-mode plasmas of JT-60U based on neutral transport simulation using the DEGAS Monte-Carlo code. A three-dimensional mesh structure including isolated dome, baffle and divertor plates is precisely built-up and the simulation space is extended from SOL to core plasma region. In this simulation background plasma parameters and the intensity of particle flux on the divertor plates are determined from the UEDGE plasma code. The dependence of plasma density on the neutral penetration and ionization area were investigated in two cases of ELMy H-mode discharge with gas puffing and without gas puffing. The simulation results showed noticeable differences in 1/e scale length in the neutral penetration and in ionization width near edge transport barrier region. Dependence of the plasma density from the pedestal edge to SOL region on the ionization region and the effect of local gas puffing are discussed in terms of neutral transport.

1. Introduction

Analysis of neutral transport is an important issue to investigate hydrogen/deuteron recycling and transport phenomena in not only the plasma edge regions but also the core plasma region of magnetically confined plasmas. Especially in improved confinement mode plasmas, neutral particles in periphery region also play a crucial role on pedestal formation near the edge transport barrier (ETB) region. Neutral particle transport simulations based on Monte-Carlo methods have been widely used as a powerful method for investigating neutral behavior in high temperature plasmas. Neutral transport codes also have been extensively utilized for the plasma transport simulation in divertor regions [1-3].

It is also an important issue to investigate the role of neutrals on the edge pedestal scaling in H-mode plasmas. So far a number of simulation studies based on the experimental data base has been extensively performed in many kinds of fusion devices and characterization of edge transport barrier in H-mode phase was investigated [4-8]. In the University of Tsukuba, the DEGAS ver.63 Monte-Carlo code has been modified for fully three-dimensional (3-D) simulation and has been applied to a tandem mirror device including non-axisymmetric cell and helical devices with non-axisymmetric magnetic configuration [9-12]. Recently 3-D neutral transport simulation using DEGAS code has been started for the study of physical mechanism of pedestal formation in the JT-60U tokamak.

In this paper, the results of neutral behavior and pedestal characteristics in H-mode plasmas are described based on the Monte-Carlo simulation using DEGAS code applied to JT-60U. In Sec. 2, a mesh structure used in the 3-D simulation is explained. Measured results in edge-pedestal region of typical ELMy H-mode discharges are described and the simulation results

of neutral penetration and ionization width are described in Sec. 3. In Sec. 4, density dependence on the ionization zone in ETB region is evaluated under the simulation results. In Sec. 5, Distinctive behavior of 3-D neutral transport in large-scale torus devices is discussed based on the simulation of local gas puffing by using 3-D DEGAS code. Finally conclusions are given in Sec. 6.

2. Mesh Model of JT-60U for DEGAS Simulation

Figure 1 shows the poloidal cross-section view of the mesh model of JT-60U for DEGAS simulation. The present mesh model is developed based on the previous one for the DEGAS2 code [3] and has a consistency with the mesh model of the UEDGE plasma code [13] has been ensured. The simulation space is also extended to the plasma core, the vacuum chamber wall and the divertor regions. The mesh is divide into 32 segments in the minor-radius direction and also divided into 28 in the azimuthal direction on the poloidal cross-section. The mesh model with 50 segments divided in the toroidal direction enables a detailed prediction of neutral density and Dα line-emission intensity and modeling of localized particle source, such as gas puffing and neutral beam injection. A benchmark test has been performed with two-dimensional simulation using DEGAS2 code and the validity of the simulation has been confirmed [14,15].

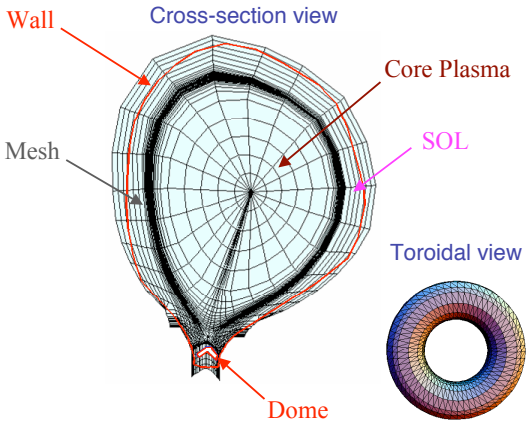

FIG. 1. Schematic drawing of the mesh model of JT-60U for DEGAS code

3. Comparison of Behavior between Discharges with Gas Puff and without Gas Puff

3.1. Plasma Parameters

In order to investigate the plasma parameter dependence on the pedestal structure, neutral transport simulation was performed in two different ELMy H-mode plasmas, and the results were compared from the viewpoint of neutral penetration and ionization region. The time behavior of plasma parameters sampled two H-mode plasma discharges is shown in Fig. 2. Between two shots, the same power of neutral beam heating is injected to the plasmas and almost the equal stored energy is obtained. In the case with gas puffing in

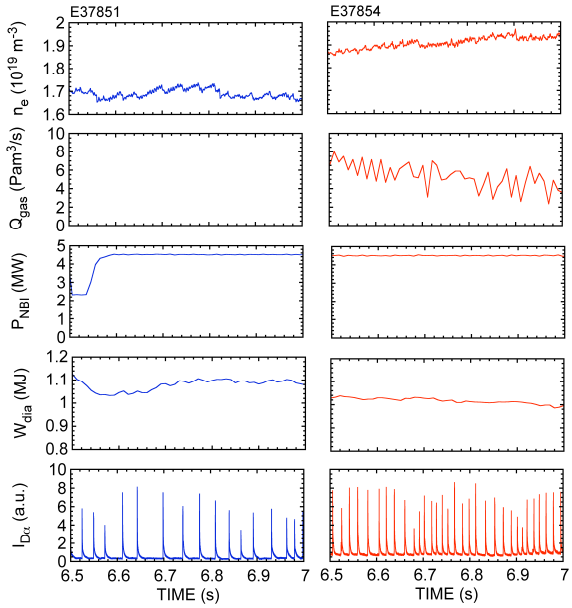

FIG. 2. Time behavior of plasma parameters in the two different ELMy H-mode plasma discharges. E37851 is the case without gas puff in the H-mode phase and E37854 represents the case with gas puff.

H-mode phase (E37851), however, relatively higher (~ 12 %) electron density is achieved than the case without gas puffing (E37854).

3.2. Edge Plasma Profile

Figure 3 shows the radial profiles of the electron density around ETB region determined from the measured data and from the UEDGE plasma code based on the obtained experimental data. These data are measured with Thomson scattering (circles) and Langmuir probes (triangles) [16,17]. In the probe data, some data, which are apparently recognized to be affected by ELM, are eliminated from the figure. Based on above these results, the spatial structure of the pedestal region was precisely investigated.

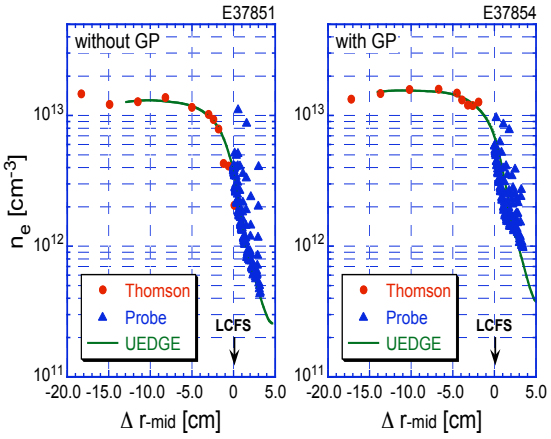

FIG. 3. Edge plasma density profiles obtained from measurements and simulation. Circles: Thomson scattering, triangles: reciprocating probe and lines: UEDGE code.

Figure 4 shows the result of the hyperbolic tangent fitting analysis in density profiles near ETB region determined from Thomson scattering measurement. From the above analysis, the determined pedestal width (distance between LCFS and the knee position) in the higher density case (E37854) is estimated to be smaller than that in the lower density case (E37851) by nearly 10 %. Based on the above input data, the neutral transport simulation with DEGAS was carried out and the penetration of neutrals is evaluated in the two H-mode plasmas.

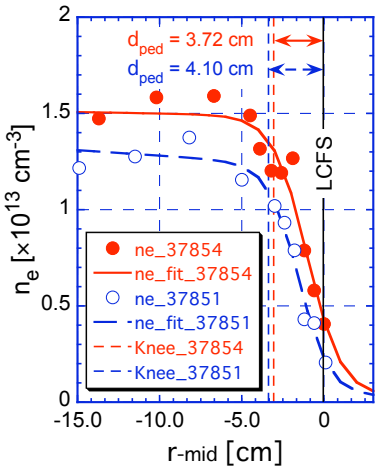

FIG. 4. Result of hyperbolic tangent fitting of density profiles in ETB region.

3.3. Simulation Results

Figure 5 shows the 2-D profile of atomic density in the poloidal cross-section determined from the DEGAS simulation for the shot E37851. In this simulation data with toroidal uniformity are used and the absolute value of the simulation results are determined by normalizing the obtained results to the measured Dα line emission intensity. Here, a particle source from the divertor

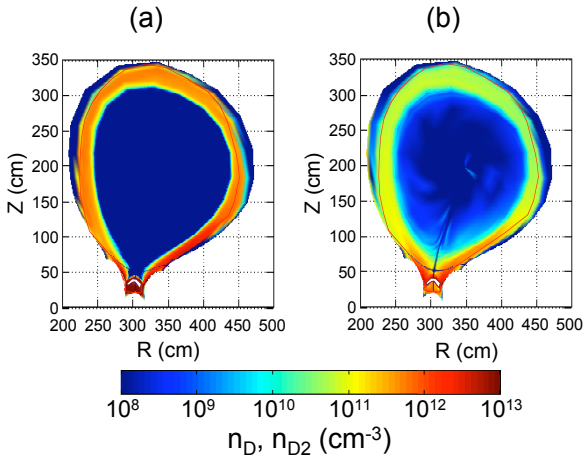

FIG. 5. Simulation result of neutral density profile. (a) deuterium molecule density, (b) deuterium atom density.

plates is dominant (4.64×10^{21} s^{-1}) compared with the others (first wall: 5.42×10^{20} s^{-1}, baffle plates: 6.22×10^{20} s^{-1}). As shown in Fig. 5(a), deuterium molecular density shows the maximum at the divertor region and decreases toward the top of the vacuum chamber by two orders of magnitude. In the radial direction into the core plasma, on the other hand, a strong reduction due to the molecular dissociation is recognized in the edge region. As shown in Fig. 5(b), the attenuation of atomic density toward the plasma core is not so strong compared with the molecules but the diffusion of atoms seems to be limited in the azimuthal direction.

3.4. Evaluation of Neutral Penetration and Ionization Zone

In Fig. 6 atomic neutral density profiles on the midplane of the plasma cross-section are plotted. There is no remarkable change in the neutral density in the SOL region. However, a noticeable increase in the decay length of atomic density is recognized in the low-density case (E37851).

By using the data from UEDGE and DEGAS, the ionization profile near the edge transport barrier region is evaluated in Fig.7. In both cases, as shown in the figure, the ionization area is localized near the LCFS and it is found that the determined width in the low-density case (#37851) is wider than those in high-density case (#37854) by 29 %. The above obtained parameter correlation among pedestal width, penetration length of neutral and ionization width in edge region is qualitatively consistent with the empirical pedestal scaling [4].

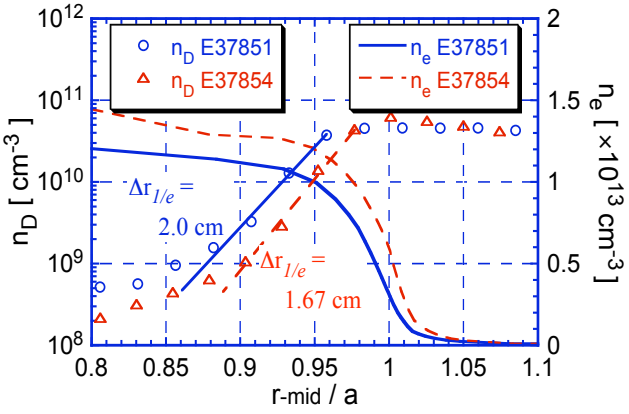

FIG. 6. Penetration of neutrals near the edge region calculated by DEGAS. Solid and dashed curves are electron density profiles. SOL density is assumed to be 1×10^{11} cm^{-3}.

4. Density Dependence on the Ionization Zone in Edge-Pedestal Region

In order to investigate the dependence of plasma density in ETB region on the ionization zone near the pedestal, the relationship between neutral penetration and ionization width is quantitatively evaluated. Figure 8 shows the density profile near ETB region given in the simulation. In this simulation, based on the density profile of the shot E37851, the density was gradually modified from the top of the pedestal (r ~ 88 cm) through to LCFS and finally changed by

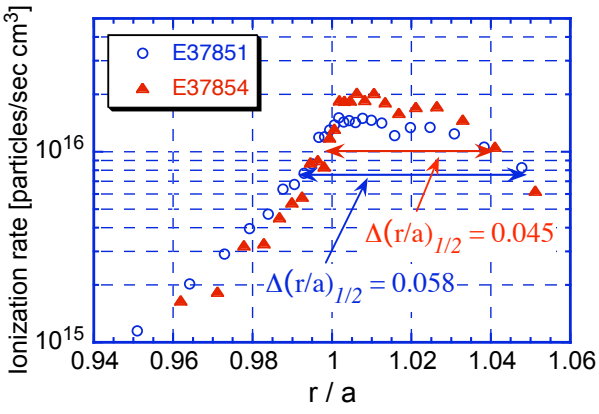

FIG. 7. Ionization profile near the edge region determined from the results of the simulation with DEGAS and UEDGE.

twice or half of the original density at the SOL region.

The simulation results are shown in Fig. 9. Deuterium molecular density shown in the upper row of the figure has no remarkable change observed in three cases. However, it is recognized that there is a slight difference in the degree of attenuation upward to the top of the vacuum chamber. On the other hand, atomic density profile shown in the middle row has a noticeable increase of the density near the divertor plates in the lower

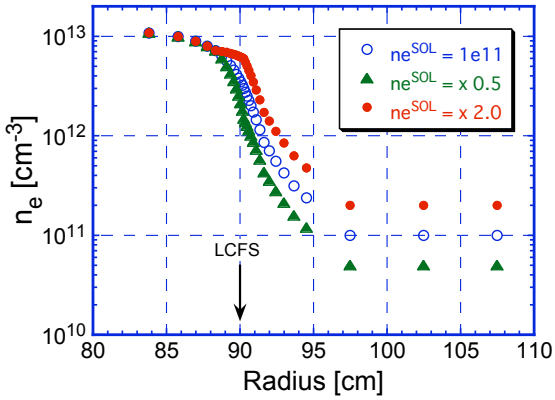

FIG. 8. The density profile near ETB region given in the simulation..

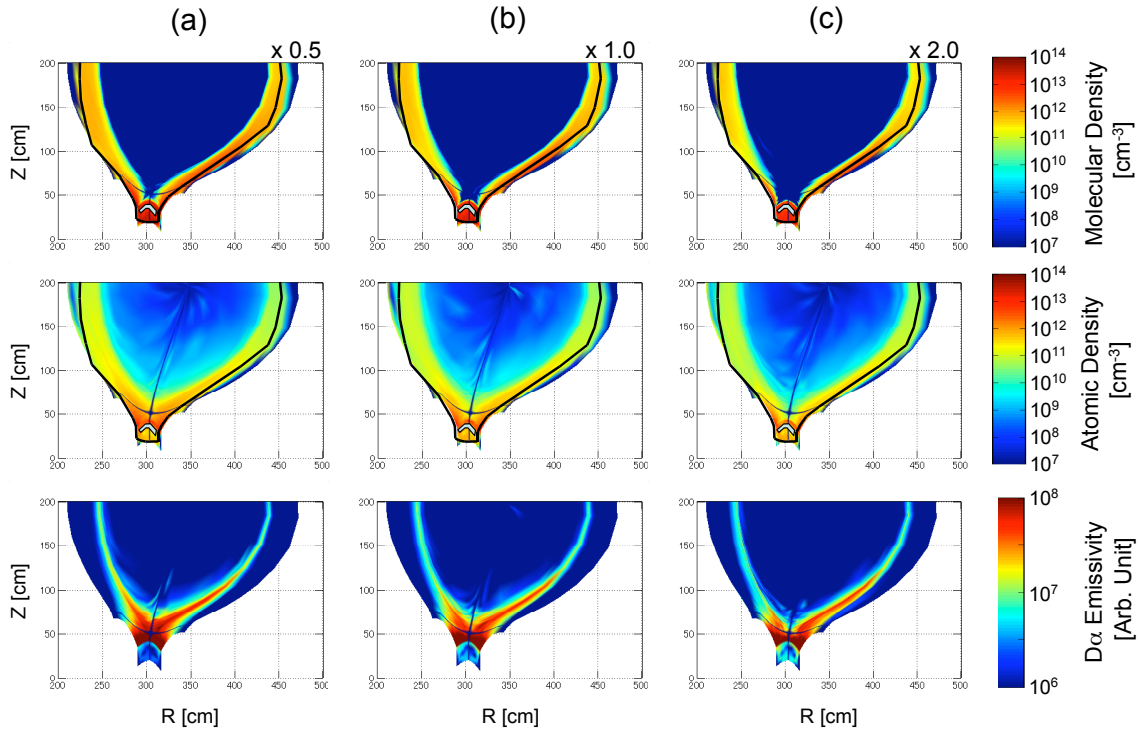

FIG. 9. 2-D cross-section view of neutral molecular and atomic densities of deuterium and Dα emissivity predicted from the DEGAS simulation. (a) ne^{SOL}= × 0.5, (b) × 1.0 (same as E37851), (c) × 2.0.

density case. This implies that the enhancement of neutral penetration occurs in this region. 2-D profile of Dα emissivity on the poloidal cross-section is calculated from the above atomic/molecular density and electron density and its temperature. It is confirmed that the clear expansion of emission area near x-point in the lower density case.

The radial profile of ionization rate determined from the simulation results is shown in Fig. 10. The ionization rate represented in the vertical axis is averaged over the poloidal direction at the same r/a position. In the SOL region, ionization rate is averaged along the open magnetic surface from the inner divertor target to the outer one. As shown in the figure, in the case of

lower density, ionization zone is shifted into the core region in accordance with its peak position. In the outer region of LCFS, on the other hand, ionization region is extended outward with the increase of density and resultant ionization width (FWHM value) becomes wider in the higher-density case.

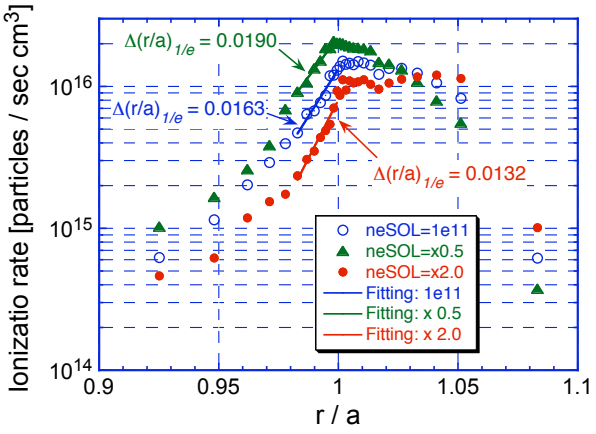

FIG. 10. Radial profile of ionization rate. Open circle: SOL density ne^{SOL} is the same as E37851, triangle: ne^{SOL}= × 0.5, filled circle: ne^{SOL} = × 2.0.

In Table I, typical parameters in the pedestal characteristics are listed in three-different density cases. The value of 1/e decay length of the ionization rate evaluated in the vicinity of LCFS ($0.98 \leq r/a \leq 1.0$) is found to be shorter in the high-density case. Above these results show a subtle discrepancy with the difference between the two discharges (E37851 and E37854), which indicates that the pedestal width may play an important role on the formation of ionization zone.

TABLE I: TYPICAL PARAMETERS IN PEDESTAL CHARACTERISTICS

Density case	ne^{SOL} (cm^{-3})	$\lambda_{1/e}^{Ionization}$ (r/a)	Ionization width (r/a)	Center of Ionization zone (r/a)
× 0.5	5×10^{10}	0.0190	0.0464	1.010
× 1.0 (E37851)	1×10^{11}	0.0163	0.0582	1.022
× 2.0	2×10^{11}	0.0132	0.0641	1.032

5. Three-Dimensional Neutral Transport in Large Tokamak Devices

Fully 3-D calculation in JT-60U tokamak was performed for the simulation of local gas puffing. In Fig. 11, neutral particle density profiles on the several poloidal cross-sections are shown in the case of D_2 gas puffing from the top of the vacuum chamber of JT-60U vacuum chamber. In this simulation, neither first-wall recycling source nor divertor source is given in order to close-up the effect of particle diffusion from the gas puff. As shown in Fig. 11(a), deuteron molecules do not penetrate into the plasma core and is observed to diffuse along the SOL to the x-point at the bottom of the chamber attenuated by more than 4 order of magnitude.

In the toroidal direction, the diffusion is faster than that of poloidal one and the reduction by only two order of magnitude is estimated at the location about 170 cm (toroidal-5) apart from the gas puffer. On the other hand, deeper penetration of atomic deuteron is observed than the case of molecules (at most several tens of magnitude) as shown in Fig. 11(b). However, there is no significant difference recognized between atoms and molecules in the poloidal direction. Figure 11(c) shows the poloidal cross-section view of Dα emissivity near the gas puffer. From this figure, it is recognized that the Dα emission area due to D_2 gas puff is limited

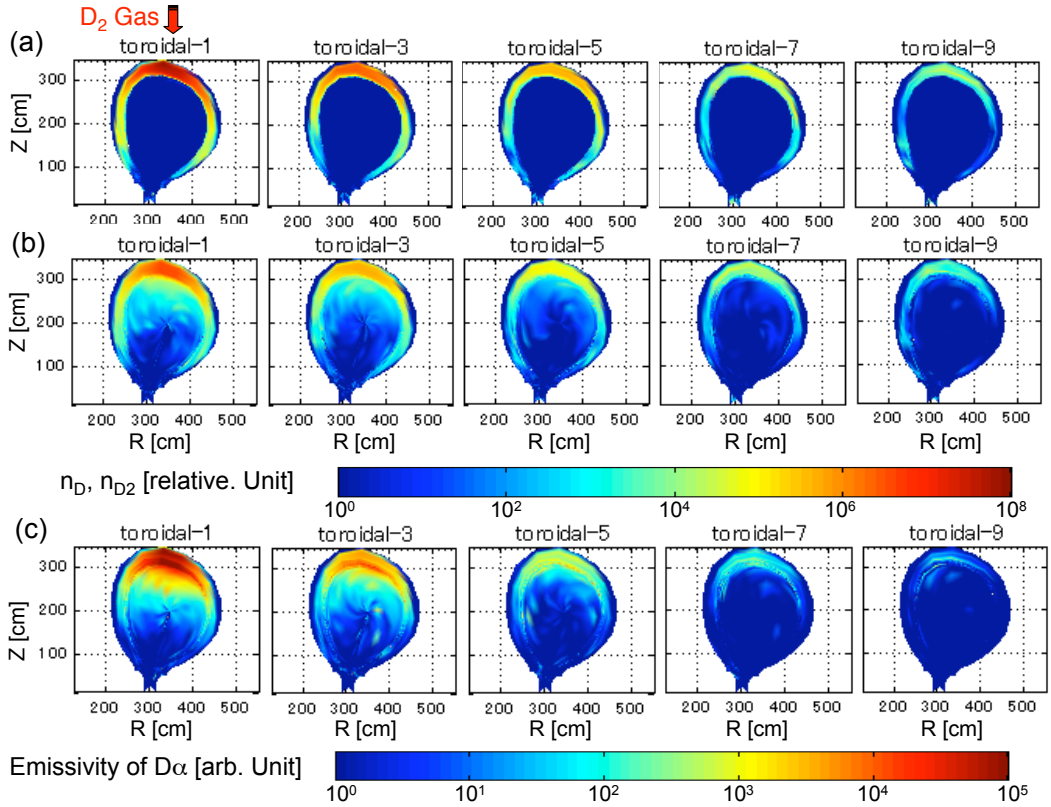

FIG. 11. Results of the 3D-DEGAS simulation in the case that the gas puffing from the top of the vacuum chamber. (a) molecular deuterium density, (b) atomic deuterium density, (c) emissivity of Dα line.

within one fifth of full torus. Therefore the first result of full 3-D neutral transport simulation indicates the significant localization of neutrals in the vicinity of the gas puff exit.

6. Conclusions

Fully 3-dimensional neutral transport simulation has been started using DEGAS Monte-Carlo code in order to investigate detailed behavior of high performance H-mode plasmas in the JT-60U tokamak. A precise mesh structure including isolated dome, baffle and divertor plates was built-up and the simulation space was extended from SOL to core plasma region. Comparison of neutral density profiles between the high and low density H-mode plasmas was carried out and the noticeable difference in neutral penetration and ionization width was recognized. The present investigation on the density dependence in pedestal and SOL regions showed that the density in the region from the pedestal to the SOL has a strong influence of neutral penetration into the core plasma region from LCFS as well as a significant effect on the ionization zone in this region. The result of 3-D simulation carried out with gas puffing showed the significant localization of neutrals around the gas puffer and the detail of neutral diffusion in toroidal and poloidal directions were clarified. The above obtained results provides the useful aspect for pedestal physics and this analysis method also gives us an important information for the three-dimensional plasma modeling in near future.

Acknowledgements

The authors would like to acknowledge the all those who contributed to the JT-60U project. This work was mainly performed based on the research collaboration between Japan Atomic Energy Agency and University of Tsukuba.

References

[1] Heifetz, D., Post, D., Petravic, M., et al., J. Comput. Phys. **46** (1982) 309.
[2] Reiter, D., et al., Plasma Phys. Contrib. Fusion **33** No.13 (1991) 1579.
[3] Stotler, D. P., et al., Contrib. Plasma Phys. **34** (1994) 392.
[4] Groebner, R. J., et al. Phys. Plasmas **9**, No.5 (2002) 2134.
[5] Kallenbach, A., et al. Plasma Phys. Control. Fusion **46** (2004) 431.
[6] Kirk, A., et al. Plasma Phys. Control. Fusion **46** (2004) A187.
[7] Horton, L. D., et al. Nucl. Fusion **45** (2005) 856.
[8] Hughes, J. W., et al. Nucl. Fusion **47** (2007) 1057.
[9] Nakashima, Y., Higashizono, Y., et al., J. Nucl. Mater. **337-339** (2005) 466.
[10] Nakashima, Y., et al., J. Plasma Phys. **72** (2006) 1123.
[11] Shoji, M., et al., J. Plasma Fusion Res. SERIES **6** (2004) 512.
[12] Kobayashi, S., et al., Proc 31th EPS conf. Plasma Phys. (London, 2004). **28G**, P-5.097.
[13] Rognlien, T. D., et al., Contr. Plasma Phys. **34** (1994) 362.
[14] Takenaga, H., et al. Nucl. Fusion **46** (2006) S39.
[15] Nakashima, Y., et al., Journal of Physics: Conference Series **123** (2008) 012029.
[16] Asakura, N., et al. Plasma Phys. Contrl. Fusion **44**. A313 (2002).
[17] Kallenbach, A., Asakura, N., et al., J. Nucl. Mater. **337-339** (2005) 381.